

ON GEOMETRIC ASPECTS OF CIRCULAR ARCS RADON TRANSFORMS FOR COMPTON SCATTER TOMOGRAPHY

T. T. Truong

Abstract If the classical line Radon transform (CLRT) has been a successful mathematical model for conventional radiation imaging modalities such as Computed Tomography (CT), Single Photon Emission Computed Tomography (SPECT) and Positron Emission Tomography (PET), the circular arc Radon transform (CART) is a potential mathematical model contender for Compton Scatter Tomography (CST). In this work we show that there are actually five classes of circular arcs on which Radon transforms can be defined and used as basis for five distinct CST modalities. These circular arcs are cut out from circles characterized by a fixed value of the power of the coordinate system origin. We also show how the five CART can be mapped onto respective CLRT, so that inversion formulas as well as some properties for function reconstruction, which are essential for working CST can be fully established.

Key words: mathematical imaging, generalized Radon transforms, Compton scatter tomography.

AMS Mathematics Subject Classification: 44A12, 45Q05, 65R10, 65R32

1 Introduction

The classical line Radon transform in \mathbb{R}^2 [1] (CLRT) has served as a mathematical model for many tomographic imaging modalities using ionizing radiation such as Computed Tomography (CT), Single Photon Emission Computed Tomography (SPECT) and Positron Emission Tomography (PET). This integral transform has been thoroughly investigated over half a century and shown to display an impressive number of properties. In imaging applications, its inversion formula provides the way to reconstruct quantities of interest, such as linear attenuation coefficient distribution in CT, gamma emitter concentration density in SPECT and beta emitter concentration density in PET.

In the mid-seventies, emerged the idea of collecting Compton scattered radiation from an object illuminated by an external source of calibrated radiation [2]. The idea made its way to the mid-nineties, when it was realized that wide angle collimators at the source as well as at the detector should be used in order to collect scattered radiation successively at various scatter energy [3]. This idea implies that the registered scattered radiation flux density at the detector is proportional to the integral of the object electron density along "isogonal" circular arcs starting from the point source and ending at the detection point. This type of *integral* measurement generalizes the integral measurement of object attenuation coefficient along propagation straight lines starting from the point source and ending at the detection point. So it is clear that,

to deal with Compton scatter tomographic imaging, there is a need to consider a new Radon transform defined on a dense set of circular arcs. We shall call it circular arc Radon transforms (CART). Of course, the set of circular arcs in the plane has a richer structure than the set of straight lines. This means that there are many distinct classes of CART. And as far as imaging processes are concerned, the CARTs are only of interest when they dispose of an explicit inversion formula. Despite an earlier attempt to adapt an inversion formula of A M Cormack [4] to a "linear" Compton scatter tomographic modality [5], which does not quite describe the process of data acquisition, there was no *bona fide* inversion formula for a realistic CST until 2010 [6, 7]. Subsequently a second CST modality based on the inversion formula of a new CART was established in 2011 [8] and discussed in [9].

The objective of this work is to present a systematic geometric approach to the CARTs, which are *relevant* for CST, in order to uncover new insights on this subject. The previous approach was successful in uncovering the relevant inversion formulas but it relies on the solutions of a determining differential equation [8]. We believe the present geometric approach to be more transparent because it is simpler and gives a unified overview of the whole question.

This paper is structured as follows. Section 2 recalls the principles of radiation tomographic imaging and shows how image formation leads to Radon transforms on straight lines and circular arcs in the plane. Section 3 reviews elementary properties of circles and circular arcs in the plane. In section 4, we introduce the definition of the CART, study the mappings of the circular arcs to corresponding straight lines and deduce the conversion of the CART into CLRT. Section 5 reports on the transfer of CLRT properties to the CART, in particular inversion formulas and orthogonal function expansions for function reconstruction. The following section 6 gives a description of the CST modalities derived from the five studied CART as well as an elegant solution to some incomplete data CST problems and suggests a multi-modal CST, capable of providing a high-quality imaging for applications. A conclusion closes the paper with some future perspectives of work.

2 Compton scatter tomography (CST)

The aim of this section is to show how an imaging process based on the mechanism of Compton scattering leads to the concept of CART.

To appreciate the originality of this imaging process, we should compare it to the conventional X-ray Computerized Tomography (CT). When a sharply collimated pencil of ionizing radiation is directed to an object, it will traverse it. But its intensity will be decreased at the detection site because of absorption in bulk matter as well as because of scattering that sends astray radiation in all directions. If the incoming radiation pencil is totally absorbed, no radiation will emerge from the scene hence it becomes totally "invisible". Scattered radiation is precisely what makes the incident radiation pencil "visible" from the side. This picture is commonly observed at optical wavelengths but not at X- or gamma wavelengths. The idea of recording this scattered radiation to reconstruct the interior of an object is what is called Compton scatter imaging. If this occurs in a slice of the object, it is termed Compton scatter tomography (CST).

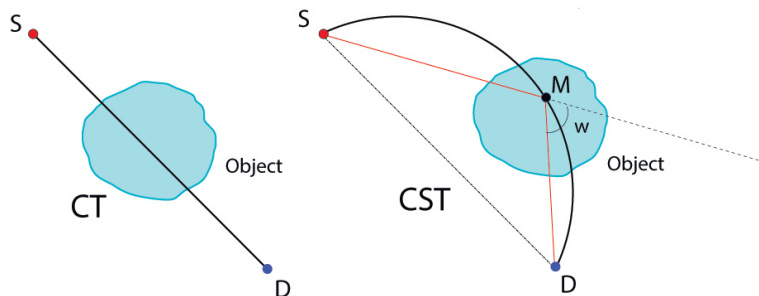


Figure 1: CT and CST respectively CLRT and CART involving respectively line and circular arc

Compton scattering of radiation by electric charges is best described in terms of photons. When an incoming X or gamma photon of energy E_0 strikes an electron at rest, it will be deflected by an angle ω , called the scattering angle (see Fig. 1), from its original direction and carries away a smaller energy $E(\omega)$, given by the so-called Compton relation

$$E(\omega) = E_0 \frac{1}{1 - \varepsilon \cos \omega}, \quad (1)$$

where $\varepsilon = E_0/mc^2$ and mc^2 is the rest energy of the electron. Unlike existing radiation tomographic modalities, which register only un-deflected photons (of energy E_0), In CST a detecting site collects the scattered photon flux density at energy $E(\omega)$. Using the Compton differential cross-section, this quantity can be expressed essentially ¹ as the integral of the scatterer (electrons) density along a circular arc starting from the point-source and ending at the detection site and subtending an angle $(\pi - \omega)$.

A scanning apparatus, called *scatterometer*, was build by Prettyman to implement this idea [10], see Fig. 2. Data on a set of isogonal circular arcs was recorded and used in image reconstruction. At the time only numerical methods for image reconstruction were applied without great success. It was realized [11] already that in order to have complete data, a set of rotated positions of the measurement device is necessary. This means that more data should be generated by rotating the *scatterometer*, bringing up the idea of a Radon transform defined on circular arcs. However, no inversion formula was available a the time and this modality has remained dormant ever since.

Our interest in CST has stemmed from the idea of S J Norton [5], who has tried to use the invertibility of the Radon transform on circles intersecting a fixed point, introduced by A M Cormack in 1964, in a particular CST modality [4], designed by him. However the electron density is integrated over the full circle. This means that scattered photons of two different energies $E(\omega)$ and $E(\pi - \omega)$ are collected in a single measurement. A correct way of getting the proper data would have limited the integration to one circular arc and leads to a CART, corresponding to one of the two scattered energies $E(\omega)$ or $E(\pi - \omega)$, as proposed in [12], but again no inversion formula was available for this case.

This situation has motivated the search for an inversion formula which can fit the working of a *rotating scatterometer*. Because of global rotational symmetry, it is

¹Apart from kinematical factors, not relevant for the mathematical problem considered here.

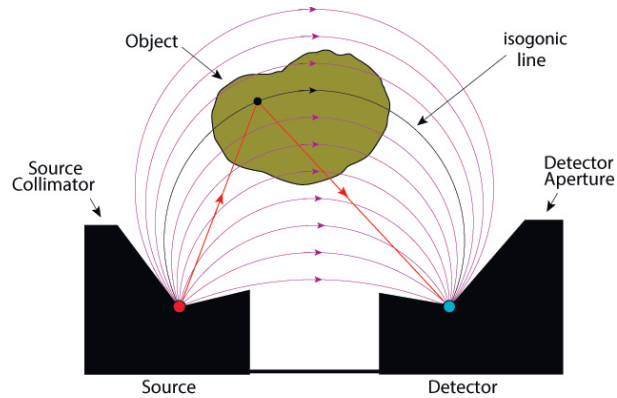


Figure 2: A sketch of Prettyman *scatterometer* [9]

convenient to work with the so-called *circular harmonic components* (or angular Fourier components) [13, 14, 15]. It was realized that, under a suitable change of variables and a change of functions, the original inversion problem can be converted into the inversion of the classical line Radon transform [6]. This elegant solution has encouraged the search for all families of curves in plane on which a Radon transform can be defined and brought back to the form of a classical line Radon transform (CLRT). This more general problem was encoded in a differential equation, which was fully solved and has led to a new CST modality [8].

In this work, we would like to use elementary geometry to present a unified structure for Radon transforms on circular arcs that are invertible by back conversion to the classical line Radon transform (CLRT). The interest lies in the fact that some of these CART are good mathematical models for CST modalities.

3 Circles and Circular Arcs in the plane

In this section we recall some elementary properties of circles and circular arcs in the plane, which are useful for the coming discussion.

3.1 The power of a point with respect to a circle

Circles in the plane depend on three parameters, *e.g.* the radius R , the two coordinates of the center Ω . Of interest are families of two-parameter circles, such as circles centered on a line or a circle, circles of fixed radius, circles going through a fixed point, etc. An alternative way to impose a constraint on the parameters is to use the concept of *power of a point with respect to a circle*, introduced by Jakob Steiner in 1830 [16] and to give it a fixed value. Without loss of generality, the point may be taken as the coordinate system origin O .

Definition 3.1. *The power of O with respect to a circle of radius R and center Ω is $\mathcal{P}_O = (O\Omega^2 - R^2)$.*

\mathcal{P}_O gives the position of O with respect to the circle, see table below.

$\mathcal{P}_O > 0$	O outside circle
$\mathcal{P}_O = 0$	O on circle
$\mathcal{P}_O < 0$	O inside circle

Then it is convenient to introduce a reference length p such that

$$\begin{aligned} \mathcal{P}_O &= \sigma p^2, \quad \text{with } \sigma = (-1, 0, 1), \\ O\Omega &= p\tau \quad \text{with } \tau > 0, \\ R &= p\sqrt{\tau^2 - \sigma}. \end{aligned} \tag{2}$$

Note that for $\sigma = 1$, one must have $\tau \geq 1$ since $R \geq 0$.

Definition 3.2. Call Γ_p the disk of radius p and centered at O .

3.2 Circle and circular arc equations

Proposition 3.3. A circle $\mathcal{C}_\sigma(p, \tau)$ of given $\mathcal{P}_O = \sigma p^2$ and center at $(O\Omega, \phi)$ has polar coordinates equation

$$\cos(\theta - \phi) = \frac{1}{2\tau} \left(\frac{r}{p} + \sigma \frac{p}{r} \right). \tag{3}$$

As $\tau > 0$, the reality of the circle requires that

$$\left| \frac{1}{2} \left(\frac{r}{p} + \sigma \frac{p}{r} \right) \right| \leq \tau. \tag{4}$$

Proof. Just write down the standard circle equation in polar coordinates (r, θ) and insert the definition of \mathcal{P}_O .

3.3 Circular arcs

In view of applications in CST, we shall be interested in circular arcs $\mathcal{C}_\sigma^\epsilon(p, \tau)$ on $\mathcal{C}_\sigma(p, \tau)$, that have end points S (the CST source site) and D (the CST detection site) on the circle boundary of Γ_p . The parameter ϵ tells whether $\mathcal{C}_\sigma^\epsilon(p, \tau)$ is exterior ($\epsilon = 1$) or interior ($\epsilon = -1$) to Γ_p . We discuss now the geometric properties of $\mathcal{C}_\sigma^\epsilon(p, \tau)$ according to the value of σ . For simplicity, we put $\gamma = (\theta - \phi)$.

Proposition 3.4. The set of all circular arcs $\mathcal{C}_\sigma^\epsilon(p, \tau)$, situated on circles $\mathcal{C}_\sigma(p, \tau)$ of fixed \mathcal{P}_O consists of three exterior ($\epsilon = 1$) and of three interior ($\epsilon = -1$) arcs with respect to Γ_p . Their equation, in polar coordinates, for all values of (σ, ϵ) , is

$$r_\sigma^\epsilon(\gamma) = p \left(\epsilon^{\frac{\sigma^2 - \sigma}{2}} (\tau \cos \gamma) + \epsilon^{\frac{\sigma^2 + \sigma}{2}} \sqrt{(\tau \cos \gamma)^2 - \sigma} \right). \tag{5}$$

The ranges of τ and γ are given in the following table, where γ_0 is the angle under which the chord SD is viewed from O .

Circular arc (σ, ϵ)	τ	γ_0	γ
$(-1, \pm 1)$	$0 < \tau < \infty$	$\pi/2$	$-\pi/2 < \gamma < \pi/2$
$(0, -1)$	$0 < \tau < 1/2$	—	$-\pi/2 < \gamma < \pi/2$
$(0, +1)$	$1/2 < \tau < \infty$	$\cos^{-1} 1/2\tau$	$-\cos^{-1} 1/2\tau < \gamma < \cos^{-1} 1/2\tau$
$(+1, \pm 1)$	$1 < \tau < \infty$	$\cos^{-1} 1/\tau$	$-\cos^{-1} 1/\tau < \gamma < \cos^{-1} 1/\tau$

Proof.

• For $\sigma = -1$, $\mathcal{P}_O < 0$ labels the two circles $\mathcal{C}_{-1}(\tau, p)$ containing the origin O inside their interior, see Fig. 3. They intersect Γ_p at points S and D situated on a diameter of Γ_p . The left-hand-side of (4), when plotted against r , shows a discontinuity at $r = p$ for $0 < r < \infty$. This curve is made up of two monotonic parts: one increasing for $0 < r < p$ and one decreasing for $p < r < \infty$.

- the interior arc $\mathcal{C}_{-1}^{-1}(p, \tau)$ has polar equation $r_{-1}^{-1}(\gamma) = p \left(\sqrt{\tau^2 \cos^2 \gamma + 1} - \tau \cos \gamma \right)$, with $0 < r_{-1}^{-1} < p$. $r_{-1}^{-1}(\gamma)$ is the positive root of $\cos \gamma = \frac{1}{2\tau} \left(\frac{p}{r} - \frac{r}{p} \right)$.

- the exterior arc $\mathcal{C}_{-1}^1(p, \tau)$ has polar equation $r_{-1}^1(\gamma) = p \left(\sqrt{\tau^2 \cos^2 \gamma + 1} + \tau \cos \gamma \right)$ with $p < r_{-1}^1 < \infty$. $r_{-1}^1(\gamma)$ is the positive root of $\cos \gamma = \frac{1}{2\tau} \left(\frac{r}{p} - \frac{p}{r} \right)$.

Here $-\pi/2 < \gamma < \pi/2$ and $0 < \tau < \infty$. We observe that the arcs $\mathcal{C}_{-1}^{\pm 1}(p, \tau)$ are inverse of each other in the circle Γ_p since $r_{-1}^1(\gamma) r_{-1}^{-1}(\gamma) = p^2$.

• For $\sigma = 0$, $\mathcal{P}_O = 0$ labels all circles $\mathcal{C}_0(p, \tau)$ passing through O , which intersects (resp. does not intersect) Γ_p if $\tau > 1/2$ (resp. if $\tau < 1/2$), see Fig. 6.

For $\tau > 1/2$, this circle intersects Γ_p at S and D separated on Γ_p by an angle $2\gamma_0 = 2 \cos^{-1}(1/2\tau)$:

- the interior arc $\mathcal{C}_0^{-1}(p, \tau)$ has the polar equation $r_0^{-1} = 2p\tau \cos \gamma$ with $(-\pi/2 < \gamma < \gamma_0) \cup (\gamma_0 < \gamma < \pi/2)$.

- the exterior arc $\mathcal{C}_0^1(p, \tau)$ has the polar equation $r_0^1 = 2p\tau \cos \gamma$, with $-\gamma_0 < \gamma < \gamma_0$.

For $0 < \tau < 1/2$, $\mathcal{C}_0(p, \tau) \cap \Gamma_p = \emptyset$, we have $r_0 = 2p\tau \cos \gamma$, with $-\pi/2 < \gamma < \pi/2$. (4) is trivially satisfied: r is always smaller than the diameter $2p\tau$.

• For $\sigma = 1$, $\mathcal{P}_O > 0$ labels circles $\mathcal{C}_1(\tau, p)$ that are orthogonal to Γ_p . They intersect Γ_p at S and D separated by an opening angle $2\gamma_0$, with $\cos \gamma_0 = \tau^{-1}$ and $\tau > 1$, see Fig. 8. SD is a chord of Γ_p . The left-hand-side of (4) for $\sigma = 1$, which is always smaller than p , is a continuous smooth curve of r which is monotonically increasing in $0 < r < p$ and monotonically decreasing in $p < r < \infty$. Each range of r corresponds successively to

- the exterior arc $\mathcal{C}_1^1(p, \tau)$ of equation $r_1^1(\gamma) = p \left(\tau \cos \gamma + \sqrt{\tau^2 \cos^2 \gamma - 1} \right)$, with $p < r_1^1 < \infty$,

- the interior arc $\mathcal{C}_1^{-1}(p, \tau)$ of equation $r_1^{-1}(\gamma) = p \left(\tau \cos \gamma - \sqrt{\tau^2 \cos^2 \gamma - 1} \right)$, with $0 < r_1^{-1} < p$.

$r_1^{\pm 1}(\gamma)$ are the two positive solutions of the equation $\cos \gamma = \frac{1}{2\tau} (r/p + p/r)$. Here $-\gamma_0 < \gamma < \gamma_0$ and $1 < \tau < \infty$. As $r_1^1(\gamma)r_1^{-1}(\gamma) = p^2$, the arcs $\mathcal{C}_1^{\pm 1}(p, \tau)$ are inverse of each other with respect to Γ_p .

Corollary 3.5. *The general expression of their line element is*

$$dl_{\mathcal{C}_\sigma^\epsilon(p, \tau)} = dr \sqrt{\frac{1 - \frac{\sigma}{\tau^2}}{1 - \frac{1}{4\tau^2} \left(\frac{r}{p} + \sigma \frac{p}{r}\right)^2}}, \quad (6)$$

which is naturally independent of ϵ .

Proof: Use $dl_{\mathcal{C}_\sigma^\epsilon(p, \tau)} = ((dr_\sigma^\epsilon(\gamma))^2 + (r_\sigma^\epsilon(\gamma) d\gamma)^2)^{1/2}$ and equation (5).

Remark 3.6. *Another class of circular arcs orthogonal to a line has been considered by V P Palamodov in [17] for seismic tomography. However they are not suitable for CST since they subtend an inscribed angle of fixed value $\pi/2$.*

4 Radon transforms on circular arcs $\mathcal{C}_\sigma^\epsilon(p, \tau)$

In view of CST, we consider Radon transforms on some of the $\mathcal{C}_\sigma^\epsilon(p, \tau)$ circular arcs. The domain of Radon transforms on $\mathcal{C}_\sigma^{-1}(p, \tau)$ (resp. $\mathcal{C}_\sigma^1(p, \tau)$) arcs, interior (resp. exterior) to Γ_p is taken to be $\mathcal{D}(\Gamma_p)$, the Schwartz space of infinitely differentiable function with compact support contained inside Γ_p (resp. $\mathcal{S}(\mathbb{R}^2 \setminus \Gamma_p)$ outside Γ_p).

4.1 Definition

Definition 4.1. *Let $f(r, \theta)$ be a smooth integrable function in an appropriate domain of \mathbb{R}^2 . The Radon transform $\mathcal{R}_{\mathcal{C}_\sigma^\epsilon(p, \tau)} f(\tau, \phi)$ of $f(r, \theta)$, for all (σ, ϵ) , is given by*

$$\mathcal{R}_{\mathcal{C}_\sigma^\epsilon(p, \tau)} f(\tau, \phi) = \int_{(r, \theta) \in \mathcal{C}_\sigma^\epsilon(p, \tau)} dl_{\mathcal{C}_\sigma^\epsilon(p, \tau)} f(r, \theta). \quad (7)$$

where dl_σ is the $\mathcal{C}_\sigma^\epsilon(p, \tau)$ arc measure (6).

In r -variable, eq. (7) reads

$$\begin{aligned} \mathcal{R}_{\mathcal{C}_\sigma^\epsilon(p, \tau)} f(\tau, \phi) = & \int_{r_{min}(\sigma, \epsilon)}^{r_{max}(\sigma, \epsilon)} dr \sqrt{\frac{1 - \frac{\sigma}{\tau^2}}{1 - \frac{1}{4\tau^2} \left(\frac{r}{p} + \sigma \frac{p}{r}\right)^2}} \times \\ & \left(f\left(r, \cos^{-1} \left(\frac{1}{2\tau} \left| \frac{r}{p} + \sigma \frac{p}{r} \right| \right) + \phi \right) + f\left(r, -\cos^{-1} \left(\frac{1}{2\tau} \left| \frac{r}{p} + \sigma \frac{p}{r} \right| \right) + \phi \right) \right). \end{aligned} \quad (8)$$

in which the integration bounds are given by

$$r_{min}(\sigma, \epsilon) = \sigma^2 p \left(\frac{1 - \epsilon}{2} \sigma (\tau - \sqrt{\tau^2 - \sigma}) + \frac{1 + \epsilon}{2} \right) + (1 - \sigma^2) p \frac{1 + \epsilon}{2}$$

(9)

$$r_{max}(\sigma, \epsilon) = \sigma^2 p \left(\frac{1 - \epsilon}{2} + \frac{1 + \epsilon}{2} (\tau + \sqrt{\tau^2 - \sigma}) \right) + (1 - \sigma^2) 2p\tau. \tag{10}$$

In equation (8), the integration variable r is actually $r_{(\sigma, \epsilon)}$.

4.2 Clue for solving the inversion problem

As far as mathematical imaging is concerned, a Radon transform without inversion formula is of no use. The aim is now to find a way to establish an inverse formula for the $\mathcal{C}_\sigma^\epsilon(p, \tau)$ circular arc Radon transforms $\mathcal{R}_{\mathcal{C}_\sigma^\epsilon(p, \tau)}$ or (CART). To this end, we follow A M Cormack's idea, who initiated the use of particular point transformations of the plane to map the posed inversion problem to the known inversion problem of the classical line Radon transform (CLRT).

Historically, A M Cormack was the first to observe that the Radon transform on circles going through the origin $\mathcal{C}_0(p, \tau)$ has the same structure as the classical Radon transform and its inversion can be obtained in a very similar way [4]. In 1981, he found two families of curves, which he called α -curves and β -curves and on which the corresponding Radon transforms have inversion formulas similar to those of the line and circle Radon transforms [18]. Later on, he also realized that because geometric inversion connects the straight line $\mathcal{L}(s, \phi)^2$ to the circle intersecting the origin $\mathcal{C}_0(p, \tau)$, as well as α -curves to β -curves, inverse formulas for related Radon transforms are also connected [19, 20]. Most importantly, he stated in [23] that the transformation

$$s \rightarrow s^\alpha \quad \text{and} \quad \theta \rightarrow (\alpha\theta), \tag{11}$$

can be used to map the Radon transform on the α -curves to the classical line Radon transform $\mathcal{R}_{\mathcal{L}(s, \phi)}$. This observation was later reiterated by in [21], where it is observed that the parabolic Radon transform can be brought back to the form of the classical Radon transform.

Here, we pursue this idea for the $\mathcal{C}_\sigma^\epsilon(p, \tau)$ arc Radon transforms by finding the appropriate point transformations of the plane which would map the $\mathcal{C}_\sigma^\epsilon(p, \tau)$ circular arcs to lines $\mathcal{L}(s, \phi)$ in the plane so that the Radon transforms on $\mathcal{C}_\sigma^\epsilon(p, \tau)$ circular arcs can be re-expressed as classical line Radon transforms. The sought geometric transforms are more general than the rigid motions of the plane, which leave the set of straight lines as well as the set of circular arcs globally invariant. Once they are found, a whole set of properties of the $\mathcal{R}_{\mathcal{C}_\sigma^\epsilon(p, \tau)}$ may be directly deduced from those of the classical line Radon transform $\mathcal{R}_{\mathcal{L}(s, \phi)}$.

² s is the distance from O to the line $\mathcal{L}(s, \phi)$ and ϕ is the angle made by the normal unit vector of $\mathcal{L}(s, \phi)$ with the Ox axis.

4.3 The radial mapping of $\mathcal{C}_\sigma^\epsilon(p, \tau)$ circular arcs to a line $\mathcal{L}_\sigma(s_\sigma, \phi)$

Definition 4.2. *Let*

$$\rho_\sigma^\epsilon = p \frac{2p r_\sigma^\epsilon}{|(r_\sigma^\epsilon)^2 + \sigma p^2|} \frac{1}{(2 - \sigma^2)}, \quad (12)$$

$$s_\sigma = \frac{p}{\tau} \frac{1}{(2 - \sigma^2)}. \quad (13)$$

Call \mathcal{T}_σ the radial mapping

$$\mathcal{T}_\sigma : r \rightarrow \rho. \quad (14)$$

Proposition 4.3. \mathcal{T}_σ is a diffeomorphism from either $(0, p)$ or (p, ∞) to either $(0, p)$ or $(0, \infty)$ mapping a $\mathcal{C}_\sigma^\epsilon(p, \tau)$ circular arc to a straight line $\mathcal{L}(s_\sigma, \phi)$ of equation

$$\rho_\sigma^\epsilon = \frac{s_\sigma}{\cos(\theta - \phi)} = \frac{s_\sigma}{\cos \gamma}, \quad (15)$$

in an auxiliary polar coordinate system (ρ, θ) , in which s_σ is its distance to the origin O and its normal unit vector makes the angle ϕ with the same fixed reference direction.

Proof. Equation (3) of the circles $\mathcal{C}_\sigma(p, \tau)$ may be put under the form of equation (15)³ using the definitions (13).

We now describe in some details the mappings \mathcal{T}_σ for later use.

4.3.1 The radial transform \mathcal{T}_{-1}

For $\sigma = -1$, equation (12) becomes

$$\rho_{-1} = p \left| \frac{2pr}{r^2 - p^2} \right|. \quad (16)$$

ρ_{-1} is a smooth function of r monotonic increasing in $[0, p[$ and monotonic decreasing in $]p, \infty[$, see Fig. 3. \mathcal{T}_{-1} is piece-wise invertible in each of these two intervals. Here p represents a physical reference length. The two $\mathcal{C}_{-1}^{\pm 1}(p, \tau)$ circular arcs subtend a common chord which is a diameter SD of Γ_p . Their polar equation, deduced from equation (5) for $\sigma = -1$, is

$$r_{-1}^{\pm 1}(\gamma) = p \left(\sqrt{\tau^2 \cos^2 \gamma + 1} \pm \tau \cos \gamma \right), \quad (17)$$

where $-\pi/2 < \gamma < \pi/2$. \mathcal{T}_{-1} maps these two circular arcs onto a straight line $\mathcal{L}(s_{-1}, \phi)$, parallel to SD , at a distance $s_{-1} = p/\tau$ from the origin O , as shown in Figures 4 and 5.

³In [8], the equations of $\mathcal{C}_{\pm 1}(p, \tau)$ circles are re-expressed as equation of $\mathcal{C}_0(p, \tau)$ circles instead of lines.

For $\tau > 1/\sqrt{3}$, the line $\mathcal{L}(s_{-1}, \phi)$ intersects the outer arc $\mathcal{C}_{-1}^1(p, \tau)$, but never intersects the inner arc $\mathcal{C}_{-1}^{-1}(p, \tau)$, see Fig. 4. The distance between the inner arc $\mathcal{C}_{-1}^{-1}(p, \tau)$ and the line $\mathcal{L}(s_{-1}, \phi)$ goes to zero only for $\tau \rightarrow \infty$. Graphically for a given γ , the intersections of a radial line with the exterior arc $\mathcal{C}_{-1}^1(p, \tau)$ and the line $\mathcal{L}(s_{-1}, \phi)$ are shown pairwise (M, M') in Figures 4. There are no intersections of the interior arc $\mathcal{C}_{-1}^{-1}(p, \tau)$ with $\mathcal{L}(s_{-1}, \phi)$, as shown in Fig. 5.

4.3.2 The radial transform \mathcal{T}_0

For $\sigma = 0$, equation (12) becomes

$$\rho_0 = \frac{p^2}{r}. \quad (18)$$

\mathcal{T}_0 is just the geometric invertible inversion in the disk Γ_p , see Fig. 11. It maps the circle $\mathcal{C}_0(p, \tau)$ of equation $r = 2\tau p \cos(\theta - \phi)$, obtained from equation (3) for $\sigma = 0$, to the straight line $\mathcal{L}(s_0, \phi)$. Here the problem has no natural basic length scale: Γ_p does not play a special role for $\mathcal{C}_0(p, \tau)$.

Hence

- for $2\tau p > p$, the circle $\mathcal{C}_0(p, \tau)$ of center $\Omega = (\tau p, \phi)$ intersects Γ_p at points S and D . The exterior arc $\mathcal{C}_0^1(p, \tau)$ is mapped onto a line segment SD internal to Γ_p at a distance $s_0 = p/2\tau < p$ from O . The interior arc $\mathcal{C}_0^{-1}(p, \tau)$ is mapped into the two half-lines, complement of SD in \mathbb{R}^2 , see Fig.11-*left*.

- for $2\tau p < p$, the circle $\mathcal{C}_0(p, \tau)$ of center $\Omega = (\tau p, \phi)$ does not intersect Γ_p , it will be transformed into a straight line intersecting $O\Omega$ at a distance $s_0 = p/2\tau > p$. Consequently each circle $\mathcal{C}_0(p, \tau)$ contained in Γ_p will be mapped onto a full straight line $\mathcal{L}(s_0, \phi)$ external to Γ_p , see Fig.11-*right*.

4.3.3 The radial transform \mathcal{T}_1

For $\sigma = 1$, equation (12) becomes

$$s_1 = \frac{p}{\tau} \quad \text{and} \quad \rho_1 = p \left(\frac{2pr}{r^2 + p^2} \right). \quad (19)$$

ρ_1 is a smooth function of r having a maximum at $r = p$ and $\rho_1 \leq p$ always. For $0 < r < p$, ρ_1 is monotonically increasing and for $p < r < \infty$, ρ_1 is monotonically decreasing, see Fig. 8.

The circle $\mathcal{C}_1(p, \tau)$ of equation

$$\cos \gamma = \frac{1}{2\tau} \left(\frac{r}{p} + \frac{p}{r} \right), \quad (20)$$

is orthogonal to Γ_p and intersecting Γ_p at S and D , see Fig. 9. The resulting circular arcs $\mathcal{C}_1^{\pm 1}(p, \tau)$ inside and outside Γ_p are given by the polar equation

$$r_1^{\pm 1}(\gamma) = p \left(\tau \cos \gamma \pm \sqrt{\tau^2 \cos^2 \gamma - 1} \right). \quad (21)$$

They are mapped by \mathcal{T}_1 onto the segment SD on the line $\mathcal{L}(s_1, \phi)$. For a given γ , the three intersections of a radial line from O with the arcs $\mathcal{C}_1^{\pm 1}(p, \tau)$ and $SD \in \mathcal{L}(s_1, \phi)$ illustrate the mapping \mathcal{T}_1 , see Fig. 9.

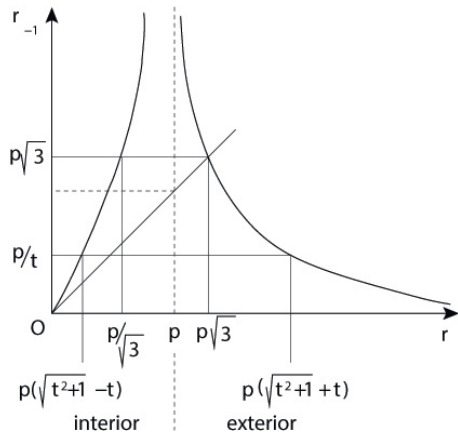


Figure 3: Transformation \mathcal{T}_{-1} : plot of ρ_{-1} against r

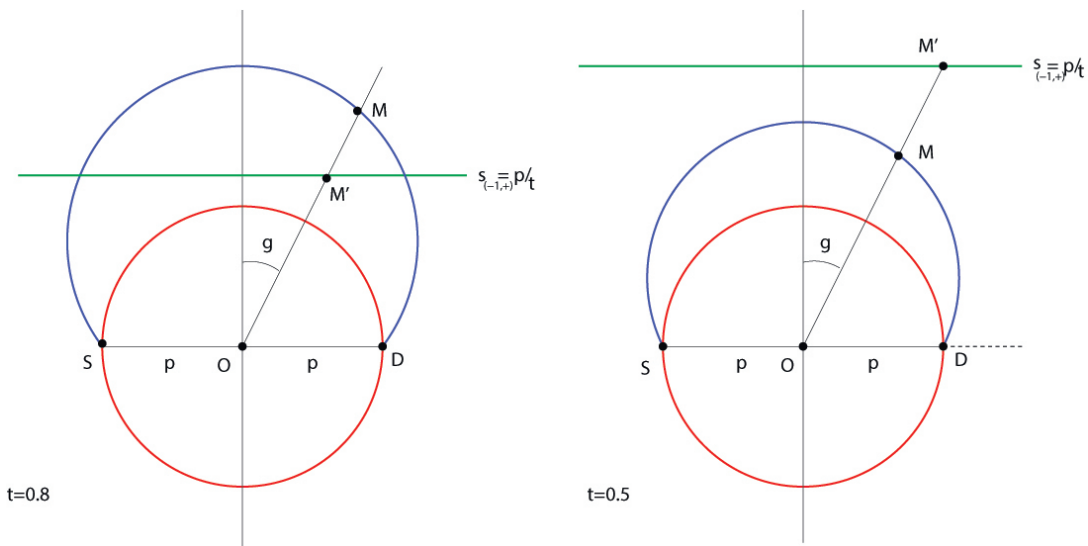


Figure 4: Transformation \mathcal{T}_{-1} : intersections of the exterior arc $\mathcal{C}_{-1}^1(p, \tau)$ with the line $\mathcal{L}(s_{-1}, \phi)$ for $\tau > 1/\sqrt{3}$ on left figure and no intersections with the exterior arc $\mathcal{C}_{-1}^1(p, \tau)$ for $\tau < 1/\sqrt{3}$ on right figure

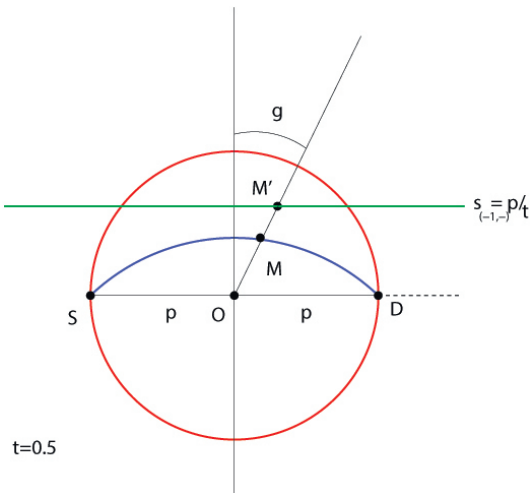
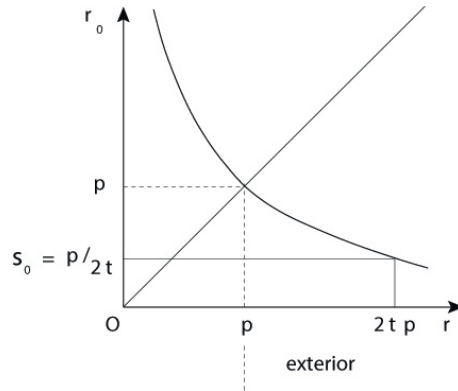
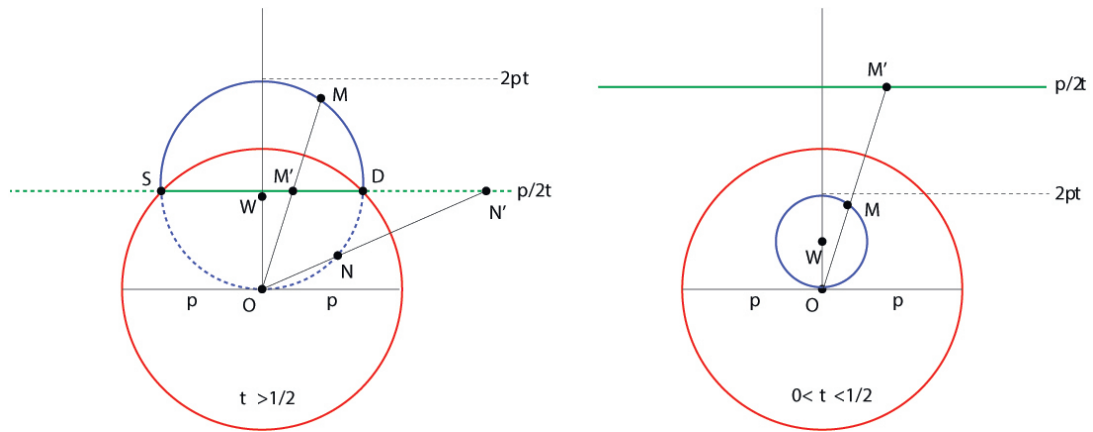


Figure 5: Transformation \mathcal{T}_{-1} : the interior arc $\mathcal{C}_{-1}^{-1}(p, \tau)$ does not intersect the line $\mathcal{L}(s_{-1}, \phi)$ for all $\tau > 0$


 Figure 6: Transformation \mathcal{T}_0 or geometric inversion: plot of ρ_0 against r

 Figure 7: Transformation \mathcal{T}_0 : relative positions of the circle $C_0(p, \tau)$ (and $C_0^{\pm 1}(p, \tau)$) with respect to the line $\mathcal{L}(s_0, \phi)$

4.4 Conversion of $\mathcal{R}_{C_0^\epsilon(p, \tau)} f(\tau, \phi)$ to a classical line Radon transforms

Theorem 4.4. For all (σ, ϵ) (except $(0, -1)$), the CART $\mathcal{R}_{C_0^\epsilon(p, \tau)} f(\tau, \phi)$ may be converted into a CLRT $\mathcal{R}_{\mathcal{L}(s_\sigma, \phi)} f(s_\sigma, \phi)$.

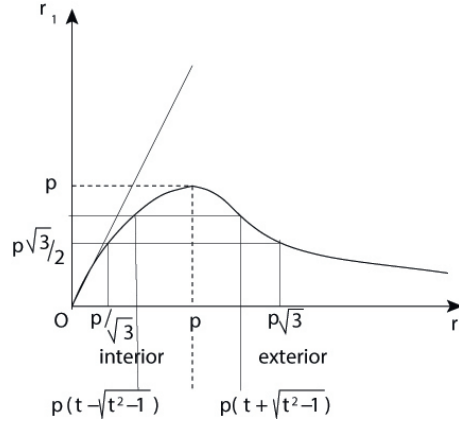
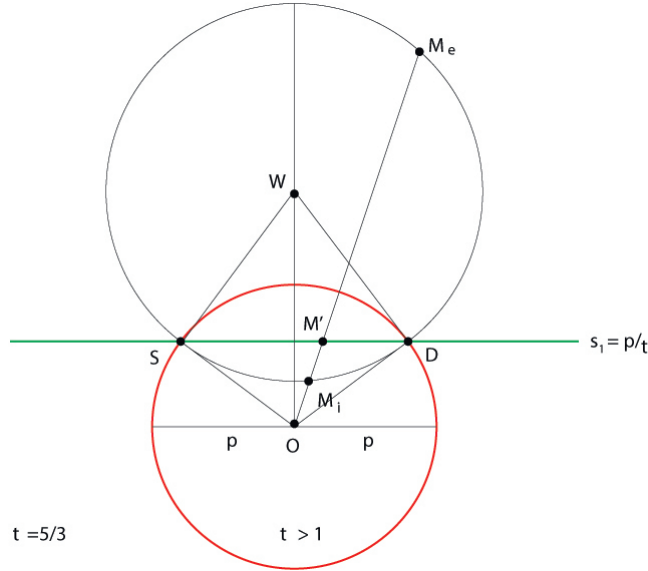
Proof. Now via the transform \mathcal{T}_σ , equation (8), giving the expression of $\mathcal{R}_{C_0^\epsilon(p, \tau)} f(\tau, \phi)$, can be rewritten as a classical line $\mathcal{L}(s_\sigma, \phi)$ Radon transform as follows.

First we reexpress $r_{(\sigma, \epsilon)}$ in terms of $\rho_{(\sigma, \epsilon)}$. This amounts to invert eq. (12)

$$\rho_{(\sigma, \epsilon)} = p \frac{2p r_{(\sigma, \epsilon)}}{|r_{(\sigma, \epsilon)}^2 + \sigma p^2|} \frac{1}{(2 - \sigma^2)}. \quad (22)$$

This operation yields

$$r_{(\sigma, \epsilon)} = p \left(\epsilon^{\frac{\sigma^2 - \sigma}{2}} \frac{p}{\rho_{(\sigma, \epsilon)}} + \epsilon^{\frac{\sigma^2 + \sigma}{2}} \sqrt{\frac{p^2}{\rho_{(\sigma, \epsilon)}^2} - \sigma} \right) \frac{1}{(2 - \sigma^2)}. \quad (23)$$

Figure 8: Transformation \mathcal{T}_1 : plot of ρ_1 against r Figure 9: Transformation \mathcal{T}_1 : intersections of the two arcs $\mathcal{C}_1^{\pm 1}(p, \tau)$ with $SD \in \mathcal{L}(s_1, \phi)$

By differentiating this equation, we obtain $dr_{(\sigma, \epsilon)}$ in terms of $d\rho_{(\sigma, \epsilon)}$

$$\frac{dr_{(\sigma, \epsilon)}}{r_{(\sigma, \epsilon)}} = -\frac{d\rho_{(\sigma, \epsilon)}}{\rho_{(\sigma, \epsilon)}} \left(\sigma^2 \frac{\frac{\epsilon p}{\rho_{(\sigma, \epsilon)}}}{\sqrt{\frac{p^2}{\rho_{(\sigma, \epsilon)}^2} - \sigma}} + (1 - \sigma^2) \right), \quad (24)$$

which is only valid for precise ranges of the parameters (σ, ϵ) . Inserting eq. (23) and eq. (24) into (8), we get

$$\begin{aligned} \mathcal{R}_{\mathcal{C}_\sigma^\epsilon(p, \tau)} f(\tau, \phi) &= \int_{\rho_l(\sigma, \epsilon)}^{\rho_u(\sigma, \epsilon)} \frac{d\rho_{(\sigma, \epsilon)}}{\rho_{(\sigma, \epsilon)}} \left(\sigma^2 \frac{\frac{\epsilon p}{\rho_{(\sigma, \epsilon)}}}{\sqrt{\frac{p^2}{\rho_{(\sigma, \epsilon)}^2} - \sigma}} + (1 - \sigma^2) \right) \sqrt{\frac{1 - \frac{\sigma}{r^2}}{1 - \frac{s_\sigma^2}{\rho_{(\sigma, \epsilon)}^2}}} \times \\ & r_{(\sigma, \epsilon)} \left(f \left(r_{(\sigma, \epsilon)}, \cos^{-1} \frac{s_\sigma}{\rho_{(\sigma, \epsilon)}} + \phi \right) + f \left(r_{(\sigma, \epsilon)}, -\cos^{-1} \frac{s_\sigma}{\rho_{(\sigma, \epsilon)}} + \phi \right) \right), \quad (25) \end{aligned}$$

where $r_{(\sigma,\epsilon)}$ is given in terms of $\rho_{(\sigma,\epsilon)}$ by equation (23), the minus sign in equation (24) has been absorbed by appropriately exchanging the order of the integration bounds, which are

$$\rho_l(\sigma, \epsilon) = \frac{p}{\tau} \frac{1 + \sigma^2}{2}, \tag{26}$$

$$\rho_u(\sigma, \epsilon) = \sigma^2 \frac{2p}{1 + \sigma} + (1 - \sigma^2) \frac{2p}{1 + \epsilon}, \tag{27}$$

and s_σ is given by equation (13). The last step consist in making a change of functions so that equation (25) appears in the form of a classical line Radon transform (CLRT).

First on the right-hand-side of equation (25), let

$$F(\rho_{(\sigma,\epsilon)}, \theta) = \frac{1}{\rho_{(\sigma,\epsilon)}} \left(\sigma^2 \frac{\epsilon p}{\sqrt{p^2 - \sigma \rho_{(\sigma,\epsilon)}^2}} + (1 - \sigma^2) \right) r(\rho_{(\sigma,\epsilon)}) f(r(\rho_{(\sigma,\epsilon)}), \theta) \tag{28}$$

and write

$$\frac{\mathcal{R}_{\mathcal{C}_\sigma^\epsilon(p,\tau)} f(\tau, \phi)}{\sqrt{1 - \frac{\sigma}{\tau^2}}} = \mathcal{R}_{\mathcal{L}(s_\sigma, \phi)} F(s_\sigma, \phi). \tag{29}$$

Then equation (25) becomes

$$\mathcal{R}_{\mathcal{L}(s_\sigma, \phi)} F(s_\sigma, \phi) = \int_{\rho_l(\sigma, \epsilon)}^{\rho_u(\sigma, \epsilon)} \frac{d\rho_{(\sigma, \epsilon)}}{\sqrt{1 - \frac{s_\sigma^2}{\rho_{(\sigma, \epsilon)}^2}} \left(F(\rho_{(\sigma, \epsilon)}, \cos^{-1} \frac{s_\sigma}{\rho_{(\sigma, \epsilon)}} + \phi) + F(\rho_{(\sigma, \epsilon)}, -\cos^{-1} \frac{s_\sigma}{\rho_{(\sigma, \epsilon)}} + \phi) \right). \tag{30}$$

This is precisely the expression of a CLRT of $F(\rho_{(\sigma,\epsilon)}, \theta)$ on line $\mathcal{L}(s_\sigma, \phi)$.

Remark 4.5. *What is established here is a \mathbb{R}^2 particular case of a more general result due to V P Palamodov in [22], where it is shown that a very large class of Radon type of integral transforms admit a reconstruction formula of the form of the classical line Radon Transform (CLRT).*

The next table shows how a $\mathcal{C}_\sigma^\epsilon(p, \tau)$ circular arc Radon transform (CART) is converted into a *specific problem* of the $\mathcal{R}_{\mathcal{L}(s, \phi)}$ classical line Radon transform (CLRT).

$\mathcal{R}_{\mathcal{C}_0^\epsilon(p,\tau)}$	$\epsilon = -1$	$\epsilon = +1$
$\sigma = -1$ $0 < \tau < \infty$	$\mathcal{R}_{\mathcal{L}(s,\phi)}$: Full plane Problem $0 < (s_{-1} \leq \rho_{-1}) < \infty$	$\mathcal{R}_{\mathcal{L}(s,\phi)}$: Full plane Problem $0 < (s_{-1} \leq \rho_{-1}) < \infty$
$\sigma = 0$ $1/2 < \tau < \infty$		$\mathcal{R}_{\mathcal{L}(s,\phi)}$: Interior Problem $0 < (s_0 \leq \rho_0) < p$
$\sigma = +1$ $1 < \tau < \infty$	$\mathcal{R}_{\mathcal{L}(s,\phi)}$: Interior Problem $0 < (s_1 \leq \rho_1) < p$	$\mathcal{R}_{\mathcal{L}(s,\phi)}$: Interior Problem $0 < (s_1 \leq \rho_1) < p$

These results will be important for function reconstruction in CART via the function reconstruction in CLRT.

Remark 4.6. For $(\sigma = 0, \epsilon = -1)$, the interior $\mathcal{C}_0^{-1}(p, \tau)$ arc is transformed by \mathcal{T}_0 (inversion in Γ_p) into the external parts (relative to Γ_p) of the straight line $\mathcal{L}(s_0, \phi)$ which intersects Γ_p , see fig. 10. To the best knowledge of the author, no information on this problem is available.

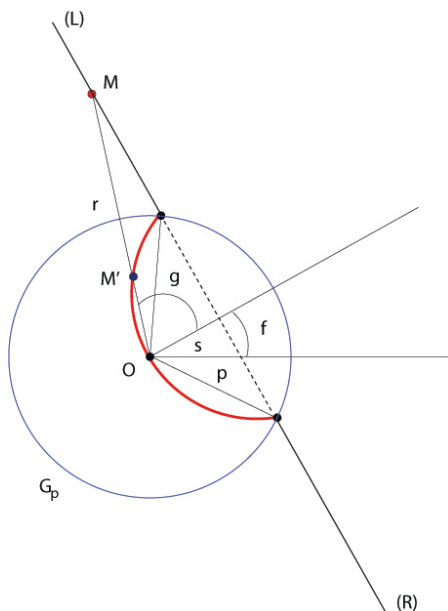


Figure 10: Inversion external half-lines into internal circular arc through O

Consequently there remains only *five* cases which are of interest for CST, for which one can transfer the main properties of the classical line Radon transform (CLRT) to the corresponding circular arc Radon transforms (CART).

4.5 A sufficient condition

We have shown the existence of five families of circular arcs on which one may defined five Radon problems that can be converted into two Radon problems: the interior and the full plane Radon problems.

We now ask the question what are the curves, having the same symmetries as the straight line, on which the expression of Radon transform can be brought back to the form of a CLRT? The answer is given by

Theorem 4.7. *A sufficient condition for the Radon transform on curves $\mathcal{C}(s, \phi)$ of polar equation $s = g(r) \cos(\theta - \phi)$, where $g(r)$ is an unknown odd function and $(s, \phi) \in \mathbb{R} \times \mathbb{S}^1$ to be brought back to the form of Radon transform on straight lines (CLRT) is*

$$\left(\frac{1}{g^2(r)} - \left(\frac{r g'(r)}{g^2(r)} \right)^2 \right) = \text{Const.} \quad (31)$$

Proof. Using the integration line element of the curve $\mathcal{C}(s, \phi)$

$$dl_{\mathcal{C}(s, \phi)} = \sqrt{1 + s^2 \left(\left(\frac{r g'(r)}{g^2(r)} \right)^2 - \frac{1}{g^2(r)} \right)} \frac{dr}{\sqrt{1 - (s/g(r))^2}}, \quad (32)$$

the Radon transform of a function $f(\rho, \theta)$ on this curve is

$$\begin{aligned} \mathcal{R}_{\mathcal{C}(s, \phi)} f(s, \phi) = \\ \int_{r_{min}}^{r_{max}} dr \frac{\sqrt{1 - s^2 H(r)}}{\sqrt{1 - (s/g(r))^2}} (f(r, \cos^{-1}(s/g(r)) + \phi) + f(r, -\cos^{-1}(s/g(r)) + \phi)), \end{aligned} \quad (33)$$

where

$$H(r) = \left(\frac{1}{g^2(r)} - \left(\frac{r g'(r)}{g^2(r)} \right)^2 \right), \quad (34)$$

and (r_{min}, r_{max}) are deduced from the curve $\mathcal{C}(s, \phi)$ equation and fixed according to desired conditions. Now compare this equation with the CLRT of $f(\rho, \theta)$ on a line $\mathcal{L}(s, \phi)$ at a distance s from the origin such that its normal unit vector makes an angle ϕ with the fixed axis Ox , which is

$$\mathcal{R}_{\mathcal{L}(s, \phi)} f(s, \phi) = \int_s^\infty \frac{d\rho}{\sqrt{1 - (s/\rho)^2}} (f(\rho, \cos^{-1}(s/\rho) + \phi) + f(\rho, -\cos^{-1}(s/\rho) + \phi)). \quad (35)$$

We see that a sufficient condition for (33) to take the form of a classical line Radon transform is that the factor $\sqrt{1 - s^2 H(g^{-1}(\rho))}$ should be *independent* of ρ , or $H(g^{-1}(\rho)) = \text{Constant}$. Since g has the dimension of a length, we put $\text{Constant} = \sigma/s$, where s is a

reference length, here chosen equal to the distance s from the straight line to the origin O for simplicity. This implies solving the equation

$$\left(\frac{1}{g^2(r)} - \left(\frac{r g'(r)}{g^2(r)} \right)^2 \right) = \frac{\sigma}{s^2}, \quad (36)$$

where $\sigma = (-1, 0, 1)$.

Lemma 4.8. *Equation (36) admits the solutions $g = g_\sigma$*

$$g_\sigma(r/s) = s \frac{(1 + \sigma^2)rs}{r^2 + \sigma s^2} \quad \text{and} \quad g_\sigma(s/r). \quad (37)$$

Proof. This equation is invariant under the substitutions

$$g \rightarrow -g \quad (38)$$

$$r \rightarrow 1/r. \quad (39)$$

Setting $h(r) = s/g(r)$, which is a dimensionless ratio, we obtain a first order separable differential equation

$$\frac{dh(r)}{\sqrt{h^2(r) - \sigma}} = \pm \frac{dr}{r}. \quad (40)$$

The solution clearly depends on only one constant and may be written under the form

$$h_\sigma(r/s) = \frac{1}{1 + \sigma^2} \left(\frac{r}{s} + \sigma \frac{s}{r} \right), \quad \text{and} \quad h_\sigma(s/r). \quad (41)$$

Hence the admissible functions g are of the type g_σ given by equation (37). This implies that the curves of equation

$$\cos(\theta - \phi) = \frac{s}{g_\sigma}, \quad (42)$$

are just the circles $\mathcal{C}_\sigma(s, \phi)$ and the line $\mathcal{L}(s, \phi)$ ⁴.

Hence combining the two theorems (4.4,4.5), we have

Theorem 4.9. *The only curves of \mathbb{R}^2 on which Radon transforms are defined and convertible to Classical Line Radon Transforms (CLRT) are circular arcs on circles of fixed value of the power of the coordinate origin O .*

5 Transfer of properties from CLTR to CART

We are now in a position to transcribe the main properties of $\mathcal{R}_{\mathcal{L}(s,\phi)}$ to those of $\mathcal{R}_{\mathcal{C}_\sigma(p,\tau)}$. Table 4.4 shows that only the *interior* and the *full plane* CLRT have to be considered. Precisely Cormack in [4, 13] has shown that the solution of the reconstruction problem for the interior and the full plane Radon transform is unique by inversion

⁴Compare with [8], where conversion from $\mathcal{R}_{\mathcal{C}_\sigma}$ with $(\sigma = \pm 1, \epsilon = \pm 1)$ to $\mathcal{R}_{\mathcal{C}_0}$ is done.

of the integral equation for function circular harmonic components (or Fourier angular components). He overlooked at the time the instability of this inversion formula. But later in [23], he produced a formula free of instabilities by including "consistency conditions". Interestingly he also indicated that the function reconstruction problem may be solved by orthogonal expansion of the function circular harmonic components, pre-signaling the so-called Singular Value Decomposition reconstruction method. In this section, we shall make use of the results on the interior and full plane CLRT to make statements on the reconstruction problem of the five cases of circular arc Radon transforms which are of interest for CST.

5.1 Support property

The Support Theorem for the CLRT states that, see *e.g.* [25], for $f \in \mathcal{S}(\mathbb{R}^2)$, if $\mathcal{R}_{\mathcal{L}(s,\phi)}f$ vanishes for all lines $\mathcal{L}(s,\phi) \in \mathbb{R}^2$ not intersecting a disk of finite radius, then the support of f is contained in this disk. The proof is due to Helgason and Ludwig based on the inversion formula of Cormack [27, 28] and Strichartz gave a proof for compactly supported f in [29].

Since only in the case $\sigma = -1$ do we have the full plane CLRT, we can state that

Proposition 5.1. *For $f \in \mathcal{S}(\mathbb{R}^2)$, if $\mathcal{R}_{\mathcal{C}_{-1}^{-1}(p,\tau)}f(p,\tau)$ vanishes on $\mathcal{C}_{-1}^{-1}(p,\tau)$ arcs with $0 < \tau_0 < \tau < \infty$, then the support of f is inside the disk of radius $p(\sqrt{1 + \tau_0^2} - \tau_0) < p$.*

For $f \in \mathcal{S}(\mathbb{R}^2)$, if (resp. $\mathcal{R}_{\mathcal{C}_{-1}^{+1}(p,\tau)}f(p,\tau)$) vanishes on $\mathcal{C}_{-1}^{+1}(p,\tau)$ arcs with $0 < \tau_0 < \tau < \infty$, then the support of f is outside the disk of radius $p < p(\sqrt{1 + \tau_0^2} + \tau_0)$.

Proof. Just apply the radial transform \mathcal{T}_{-1} to the CRLT Support Theorem.

Remark 5.2. *Compare with [26], who treats the case of Radon transform on circles centered on a fixed circle.*

5.2 Range characterization

The range of the CLRT is fully characterized by the theorem of Helgason-Ludwig [27, 28]. An equivalent form of this theorem has been formulated by A M Cormack in [23] as *consistency conditions* on the circular harmonic components $(\mathcal{R}_{\mathcal{L}(s,\phi)}f)_l(r)$ of $\mathcal{R}_{\mathcal{L}(s,\phi)}f(s,\phi)$, the CLRT of $f(r,\theta)$ in the full plane. Note that usually $f(\rho,\theta)$ is the transcription of a function $f^{\natural}(x,y) = f^{\natural}(\rho \cos \theta, \rho \sin \theta)$, which is 2π -periodic and expandable in θ -Fourier series. Now the circular harmonic components $f_l(r)$ (resp. $(\mathcal{R}_{\mathcal{C}_{-1}^{\epsilon}(p,\tau)}f)_l(\tau)$) of $f(r,\theta)$ (resp. $\mathcal{R}_{\mathcal{C}_{-1}^{\epsilon}(p,\tau)}f(p,\tau)$) are given by

$$f(r,\theta) = \sum_{l \in \mathbb{Z}} f_l(r) e^{il\theta} \quad \text{and} \quad \mathcal{R}_{\mathcal{C}_{-1}^{\epsilon}(p,\tau)}f(p,\tau) = \sum_{l \in \mathbb{Z}} (\mathcal{R}_{\mathcal{C}_{-1}^{\epsilon}(p,\tau)}f)_l(\tau) e^{il\theta}. \quad (43)$$

Then equation (8) is replaced by the radial Radon integral equation (RRIE)

$$(\mathcal{R}_{\mathcal{C}_{-1}^{\epsilon}(p,\tau)}f)_l(\tau) =$$

$$\int_{r_{min}(-1,\epsilon)}^{r_{max}(-1,\epsilon)} dr \sqrt{\frac{1 + \frac{1}{\tau^2}}{1 - \frac{1}{4\tau^2} \left(\frac{r}{p} - \frac{p}{r}\right)^2}} \cos\left(l \cos^{-1}\left(\frac{1}{2\tau} \left|\frac{p}{r} - \frac{r}{p}\right|\right)\right) f_l(r), \quad (44)$$

where the integration boundaries are given by equations (9,10). Hence for the case $\sigma = -1$, a range consistency condition can be derived for the CART from that of the CLRT, as

Proposition 5.3. *The $\mathcal{R}_{\mathcal{C}_{-1}^\epsilon}$ of a function $f \in \mathcal{S}(\mathbb{R}^2)$ satisfies the condition*

$$\int_0^\infty \frac{d\tau}{\tau} \left(\frac{p}{\tau} \frac{1}{2 - \sigma^2}\right)^{k+1} \frac{\left(\mathcal{R}_{\mathcal{C}_{-1}^\epsilon} f(\tau)\right)_l}{\sqrt{1 - (\sigma/\tau)^2}} = 0 \quad (45)$$

for $k = l - 2, l - 4, \dots, > -1$.

Proof. Use of known results for CLRT [23]:

$$\int_0^\infty ds s_{-1}^m (\mathcal{R}_{\mathcal{L}(s_{-1}, \phi)} f)_l(s_{-1}) = 0,$$

for $m = l - 2, l - 4, \dots, > -1$, with $s_{-1} = p/\tau$ and equation (29).

5.3 Null space

Proposition 5.4. *The null space of $\mathcal{R}_{\mathcal{C}_{-1}^\epsilon}$ consists of the linear span of*

$$f_l^k(r) = \frac{\sqrt{p^2 + \rho_{(-1,\epsilon)}^2}}{\epsilon p r (\rho_{(-1,\epsilon)})^{k-1}}. \quad (46)$$

where $\rho_{(\sigma,\epsilon)}$ given in terms of r by equation (12).

Proof. The null space of $\mathcal{R}_{\mathcal{L}(s,\phi)} f(s, \phi)$ are known from Perry's work [30]: functions with circular harmonic component $1/r^k$ have zero CLRT

$$\left(\mathcal{R}_{\mathcal{L}(s,\phi)} f\right)_l(s) = 2 \int_s^\infty dr \frac{\cos(l \cos^{-1}(s/r))}{\sqrt{1 - (s/r)^2}} \frac{1}{r^k} = 0, \quad (47)$$

if $k = l - 2, l - 4, \dots, > -1$. This implies that the null space of CLRT is the linear span of these r^{-k} . Then use equation (28) to get the result.

5.4 Reconstruction of functions for the CART with $\sigma = -1$

This Radon transform on exterior and interior $\mathcal{C}_{-1}^\epsilon(p, \tau)$ circular arcs is mapped onto the *full plane* Radon transform on the line $\mathcal{L}((p/\tau), \phi)$, which has a closed form free of instabilities reconstruction formula, given in [32, 23]. After transcription into our notations, it reads

$$F(\rho_{(-1,\epsilon)}, \theta) = \frac{1}{2\pi} \int_0^{2\pi} d\phi \int_0^\infty d\tau \frac{1}{s_{-1} - \rho_{(-1,\epsilon)} \cos(\theta - \phi)} \frac{\partial}{\partial \tau} \mathcal{R}_{\mathcal{L}(s_{-1}, \phi)} f(s_{-1}, \phi). \quad (48)$$

The τ integration is understood as a principal value. Now using equations (22) and (28) to re-express $\rho_{(-1,\epsilon)}$ and $F(\rho_{(-1,\epsilon)}, \theta)$ in terms of $r_{(-1,\epsilon)}$ and $f(r_{(-1,\epsilon)}, \theta)$ we get a full closed form reconstruction formula for the $\mathcal{R}_{\mathcal{C}_{-1}^{\epsilon}(p,\tau)}$ CART transform

$$f(r_{(-1,\epsilon)}, \theta) = \epsilon \frac{p}{\pi} \frac{p^2 + r_{(-1,\epsilon)}^2}{|p^2 - r_{(-1,\epsilon)}^2|} \int_0^{2\pi} d\phi \int_0^\infty d\tau \frac{1}{\frac{1}{\tau} - \frac{2pr_{(-1,\epsilon)}}{|p^2 - r_{(-1,\epsilon)}^2|} \cos(\theta - \phi)} \frac{\partial}{\partial \tau} \frac{\tau \mathcal{R}_{\mathcal{C}_{-1}^{\epsilon}}(\tau, \phi)}{\sqrt{1 + \tau^2}}. \quad (49)$$

In his paper [4], Cormack showed that the function reconstruction problem for the full plane classical line Radon transform can be solved also by orthogonal expansion techniques, which are the building blocks of the Singular Value Decomposition (SVD) method for operators in Hilbert spaces. Here we shall not go into the details of the SVD theory, which is detailed in [34], but simply give the orthogonal functions for the expansion of the circular harmonic components $f_l(r)$ and $(\mathcal{R}_{\mathcal{C}_s^{\epsilon}(p,\tau)} f)_l(\tau)$.

5.4.1 CLRT

For this task, we recall the orthogonal systems given by A M Cormack for the full plane CLRT $\mathcal{R}_{\mathcal{L}(s,\phi)} f(s, \phi)$. He made the choice of input circular harmonic component $F_l(\rho)$ of some function $F(\rho, \phi)$, see [4]

$$F_l(\rho) = S_l^k(\rho) = \rho^l L_k^l(\rho^2), \quad (50)$$

where $L_k^l(x)$ is a generalized Laguerre polynomial, see [31], with the orthogonality relation

$$\int_0^\infty \rho d\rho e^{-\rho^2} S_l^k(\rho) S_l^{k'}(\rho) = \delta_{kk'} \frac{(l+k)!}{k!}. \quad (51)$$

Therefore $F_l(\rho)$ may be expanded as

$$F_l(\rho) = \frac{e^{-\rho^2}}{\sqrt{\pi}} \sum_{k'=0}^{\infty} (-1)^{l+k'} 2^{l+2k'} k'! a_l^{k'} S_l^{k'}(\rho), \quad (52)$$

where $a_l^{k'}$ are the coefficients to be determined from the data.

Now the CLRT radial Radon integral transform of $e^{-\rho^2} S_l^k(\rho)$ is

$$\begin{aligned} & \left(\mathcal{R}_{\mathcal{L}(s,\phi)} e^{-\rho^2} S_l^k(\rho) \right) (s) = \\ & 2 \int_s^\infty d\rho \frac{\cos(l \cos^{-1} s/\rho)}{\sqrt{1 - (s/\rho)^2}} e^{-\rho^2} S_l^k(\rho) = \frac{(-1)^{l+k} \sqrt{\pi}}{k! 2^{l+2k}} e^{-s^2} H_{l+2k}(s). \end{aligned} \quad (53)$$

The Hermite polynomials $H_n(s)$ verify the following orthogonality relation

$$\int_0^\infty ds e^{-s^2} H_k(s) H_{k'}(s) = \delta_{kk'} \frac{\sqrt{\pi}}{2} 2^k k!, \quad (54)$$

where k and k' must be of same parity. Hence the CLRT of $F_l(\rho)$ takes the form

$$(\mathcal{R}_L F)_l(s) = e^{-s^2} \sum_{k=0}^{\infty} a_l^k H_{l+2k}(s). \quad (55)$$

This means that the expansion coefficient a_l^k may be obtained from the projection of the Radon data on a Hermite polynomial

$$a_l^k = \frac{1}{\sqrt{\pi} 2^{l+2k} (k+2l)!} \int_{-\infty}^{\infty} ds H_{l+2k}(s) (\mathcal{R}_L F)_l(s). \quad (56)$$

Finally by putting the computed a_l^k in equation (52), one reconstruct $F_l(\rho)$ first and then reconstruct $F(\rho, \theta)$ as an angular Fourier series.

5.4.2 CART

From these results, we can now derive the orthogonal functions for the $\mathcal{R}_{C_{-1}^\epsilon}$ Radon problem. This is done by replacing ρ in the previous equations by $\rho_{(-1, \epsilon)}$

$$\rho_{(-1, \epsilon)} = p \frac{2p r_{(-1, \epsilon)}}{|r_{(-1, \epsilon)}^2 - p^2|}, \quad (57)$$

and work out the new orthogonality integration measure using

$$d\rho_{(-1, \epsilon)} = -\epsilon \frac{2p^2 (r^2 + p^2)}{|r^2 - p^2|^2} dr_{(-1, \epsilon)}. \quad (58)$$

The orthogonal system to be chosen is $S_l^k(\rho_{(-1, \epsilon)})$, which satisfies the orthogonality relation

$$\begin{aligned} \int_{p/(1+\epsilon)/2}^{2p/(1-\epsilon)} \frac{2p^2 (r^2 + p^2)}{|r^2 - p^2|^2} dr_{(-1, \epsilon)} e^{-\left(p \frac{2p r_{(-1, \epsilon)}}{|r_{(-1, \epsilon)}^2 - p^2|}\right)^2} S_l^k\left(p \frac{2p r_{(-1, \epsilon)}}{|r_{(-1, \epsilon)}^2 - p^2|}\right) S_l^{k'}\left(p \frac{2p r_{(-1, \epsilon)}}{|r_{(-1, \epsilon)}^2 - p^2|}\right) \\ = \delta_{kk'} \frac{(l+k)!}{k!}, \end{aligned} \quad (59)$$

with the weight $\exp - \left(p \frac{2p r_{(-1, \epsilon)}}{|r_{(-1, \epsilon)}^2 - p^2|}\right)^2$.

The reconstruction of $f_l(r_{(-1, \epsilon)})$ follows the same pattern as for $F_l(\rho)$: expansion of $f_l(r_{(-1, \epsilon)})$ in terms of $S_l^k\left(p \frac{2p r_{(-1, \epsilon)}}{|r_{(-1, \epsilon)}^2 - p^2|}\right)$ with a pre-factor $e^{-\left(p \frac{2p r_{(-1, \epsilon)}}{|r_{(-1, \epsilon)}^2 - p^2|}\right)^2}$ as in equation (52). Then the $\mathcal{R}_{C_{-1}^\epsilon}$ Radon transform of $S_l^k\left(p \frac{2p r_{(-1, \epsilon)}}{|r_{(-1, \epsilon)}^2 - p^2|}\right)$ is the Hermite polynomial $H_{l+2k}(p/\tau)$, which obeys the orthogonality relation

$$\int_0^\infty ds \frac{p}{\tau^2} e^{-(p/\tau)^2} H_k(p/\tau) H_{k'}(p/\tau) = \delta_{kk'} \frac{\sqrt{\pi}}{2} 2^k k!. \quad (60)$$

Inverting equation (28) for $\sigma = -1$, and replacing $\rho_{(-1,\epsilon)}$ in terms of $r_{(-1,\epsilon)}$ using equation (22) also for $\sigma = -1$, we have

$$f(r_{(-1,\epsilon)}, \theta) = \epsilon \frac{2p(r_{(-1,\epsilon)}^2 + p^2)}{(r_{(-1,\epsilon)}^2 - p^2)^2} \sum_{l=-\infty}^{\infty} F_l \left(p \frac{2pr_{(-1,\epsilon)}}{|r_{(-1,\epsilon)}^2 - p^2|} \right) e^{il\theta}, \quad (61)$$

with the expansion

$$F_l \left(p \frac{2pr_{(-1,\epsilon)}}{|r_{(-1,\epsilon)}^2 - p^2|} \right) = \frac{1}{\sqrt{\pi}} e^{-\left(p \frac{2pr_{(-1,\epsilon)}}{|r_{(-1,\epsilon)}^2 - p^2|} \right)^2} \sum_{k=0}^{\infty} (-1)^{l+k} 2^{l+2k} k! b_l^k S_l^k \left(p \frac{2pr_{(-1,\epsilon)}}{|r_{(-1,\epsilon)}^2 - p^2|} \right), \quad (62)$$

where the expansion coefficient b_l^k is obtained as

$$b_l^k = \frac{2}{\sqrt{\pi} 2^{l+2k} (k+2l)!} \int_0^{\infty} d\tau \frac{p}{\tau^2} (\mathcal{R}_{\mathcal{L}(p/\tau, \phi)} F)_l(p/\tau). \quad (63)$$

The reconstruction by orthogonal expansion for $\sigma = -1$ is therefore completed.

5.5 Reconstruction of functions for the CART with $\sigma = 0, 1$

The table of theorem 4.4 shows that these two CART are mapped onto the *interior* problem of the CLRT. The same procedure as in previous subsection is applied. We give first the orthogonal functions for the radial CLRT, which are slightly different from those of A M Cormack [24].

The radial orthogonal system consists of the generalized Zernike polynomials $\overline{R}_l^{k,\lambda}(\rho)$ which are defines as

$$\overline{R}_l^{k,\lambda}(\rho) = \rho^l (1 - \rho^2)^{\lambda-1} \frac{\Gamma(l+2k+\lambda)}{k!(l+k)!} G_k(l+\lambda, l+1; \rho^2), \quad (64)$$

where $G_k(l+\lambda, l+1; \rho^2)$ are the shifted argument Jacobi polynomials of Courant-Hilbert, see [31]. This choice is made to coincide with the radial Zernike polynomials for $\lambda \rightarrow 1$. Their orthogonality relation is

$$\int_0^1 \frac{\rho d\rho}{(1-\rho^2)^{\lambda-1}} \overline{R}_l^{k,\lambda}(\rho) \overline{R}_l^{k',\lambda}(\rho) = \delta_{kk'} \frac{1}{2(l+2k+\lambda)} \frac{\Gamma(l+k+\lambda)}{(l+k)!} \frac{\Gamma(k+\lambda)}{k!}. \quad (65)$$

Their radial Radon transforms are Gegenbauer polynomials

$$\begin{aligned} & \left(\mathcal{R}_{\mathcal{L}(s, \phi)} \overline{R}_l^{k,\lambda} \right)_l(s) = \\ & (-i)^l (-1)^{\frac{|l|}{2}} 2^{2\lambda-2} B(k+\lambda, l+k+\lambda) \frac{\Gamma(\lambda)}{(k!)^2} (1-s^2)^{\lambda-1/2} C_{l+2k}^\lambda(s), \end{aligned} \quad (66)$$

where $B(x, y)$ is the Euler beta function and $C_{l+2k}^\lambda(s)$ are Gegenbauer polynomials with their corresponding orthogonality relation

$$\int_0^1 ds (1-s^2)^{\lambda-(1/2)} C_l^\lambda(s) C_{l'}^\lambda(s) = \frac{1}{2} \delta_{ll'} \frac{\pi 2^{1-2\lambda} \Gamma(l+2\lambda)}{l! (\lambda+l) [\Gamma(\lambda)]^2}, \quad (67)$$

for l and l' either odd or even. We are in a position to treat the two cases $\sigma = 0, 1$.

From now on, to simplify notations we set $p = 1$ and give the corresponding orthogonal expansions for $\sigma = 0, 1$ and $\epsilon = \pm 1$.

5.5.1 Case $\sigma = 0, \epsilon = 1$

We substitute first $\rho_0 = 1/r_{(0,1)}$ into equation (65) and get the orthogonality relation in terms of $r_{(0,1)}$

$$\int_1^\infty \frac{dr_{(0,1)}}{r_{(0,1)}^2 (r_{(0,1)}^2 - 1)^{\lambda-1}} \overline{R}_l^{k,\lambda}(1/r_{(0,1)}) \overline{R}_l^{k',\lambda}(1/r_{(0,1)}) = \delta_{kk'} \frac{1}{2(l+2k+\lambda)} \frac{\Gamma(l+k+\lambda)}{(l+k)!} \frac{\Gamma(k+\lambda)}{k!}. \quad (68)$$

We now set $s_0 = 1/2\tau$ in equation (67)

$$\int_1^\infty \frac{d\tau}{2\tau^2} (1 - (1/4\tau)^2)^{\lambda-(1/2)} C_l^\lambda(1/2\tau) C_{l'}^\lambda(1/2\tau) = \frac{1}{2} \delta_{ll'} \frac{\pi 2^{1-2\lambda} \Gamma(l+2\lambda)}{l! (\lambda+l) [\Gamma(\lambda)]^2}. \quad (69)$$

5.5.2 Case $\sigma = 1, \epsilon = \pm 1$

We substitute first $\rho_1 = \frac{2r_{(1,\epsilon)}}{1+r_{(1,\epsilon)}^2}$ into equation (65) and get the orthogonality relation in terms of $r_{(1,\epsilon)}$. The orthogonality relation (65) becomes now

$$\int_0^1 r_{(1,\epsilon)} dr_{(1,\epsilon)} \frac{(1+r_{(1,\epsilon)}^2)^{2\lambda-5}}{(1-r_{(1,\epsilon)}^2)^{2\lambda-3}} \overline{R}_l^{k,\lambda}\left(\frac{2r_{(1,\epsilon)}}{1+r_{(1,\epsilon)}^2}\right) \overline{R}_l^{k',\lambda}\left(\frac{2r_{(1,\epsilon)}}{1+r_{(1,\epsilon)}^2}\right) = \frac{1}{4} \delta_{kk'} \frac{1}{2(l+2k+\lambda)} \frac{\Gamma(l+k+\lambda)}{(l+k)!} \frac{\Gamma(k+\lambda)}{k!}, \quad (70)$$

with $s_0 = 1/\tau$ and consequently

$$\int_1^\infty \frac{d\tau}{\tau^2} (1 - (1/\tau)^2)^{\lambda-(1/2)} C_l^\lambda(1/\tau) C_{l'}^\lambda(1/\tau) = \frac{1}{2} \delta_{ll'} \frac{\pi 2^{1-2\lambda} \Gamma(l+2\lambda)}{l! (\lambda+l) [\Gamma(\lambda)]^2}. \quad (71)$$

6 Applications of CART to CST

6.1 Five CST modalities arising from five CART

As mentioned in the introduction, a two-parameter family of circular arcs among the five studied above may serve to define a CST modality. The calibrated mono-energetic radiation source is at the end S of the circular arc and the detection site D is at its other end point. For the $\sigma = -1$ -modality, S and D are on a rotating diameter of Γ_p . But for the $\sigma = (0, 1)$ -modalities, S and D are moving on the circle boundary of Γ_p ,

separated by an angle $2\gamma_0 < \pi$. The five CST modalities are specified by the range of the Compton scattering angle ω given by the following table in terms of the geometric parameter τ , the opening angle γ_0 .

Arc (σ, ϵ)	τ	γ_0	$\omega(\epsilon = -1)$	$\omega(\epsilon = +1)$	s_σ
$(-1, \pm 1)$	$0 < \tau < \infty$	$\pi/2$	$\omega = \cot^{-1} \tau$ $0 < \omega < \pi/2$	$\omega = -\cot^{-1} \tau$ $\pi/2 < \omega < \pi$	$s_{-1} = p \tan \omega $
$(0, +1)$	$1/2 < \tau < \infty$	$\cos^{-1} 1/2\tau$		$\omega = 2\gamma_0$ $0 < \omega < \pi$	$s_0 = p \cos(\omega/2)$
$(+1, \pm 1)$	$1 < \tau < \infty$	$\cos^{-1} 1/\tau$	$\omega = \pi/2 - \gamma_0$ $0 < \omega < \pi/2$	$\omega = \gamma_0 + \pi/2$ $\pi/2 < \omega < \pi$	$s_1 = p \sin \omega$

Three modalities with $(\sigma = -1, +1, 0, \epsilon = 1)$ are particularly suited for large objects, the scanning being done on one side (in particular on objects immersed in a medium), as in [5, 33], see Figures 11 and 12. For small objects, there are two scanning modalities with $(\sigma = \pm 1, \epsilon = -1)$ which can accommodate a circular radiation shielding belt, see Figures 13. They may be suited for medical imaging.

6.2 Solving indirectly the incomplete data problem for the CART

6.2.1 In $(\sigma = -1, \epsilon = -1)$ CST modality

The table in theorem 4.4 shows that the full $\mathcal{R}_{\mathcal{C}_{-1}^{-1}(p, \tau)}$ corresponds to the full plane $\mathcal{R}_{\mathcal{L}(s, \phi)}$ problem: because $s_{-1} = p \tan \omega$ with $0 < \omega < \pi/2$, we have $0 < s_{-1} < \infty$. Now it is observed that for small scattering angles ω (or $\tau = \cot \omega$), data acquisition is problematic and a cut-off ω_0 (or $\tau_0 = \cot \omega_0$) must be set up. Then the corresponding CLRT problem is just the *exterior* CLRT problem, for which Perry has given a solution [30]. Thus we get the surprising result that the circular arc Radon transform in an annulus (or radii p and $p(\sqrt{1 + \tau^2} - \tau) < p$) has an exact inversion solution by orthogonal functions expansion. See left image of Fig. 14.

6.2.2 In $(\sigma = -1, \epsilon = 1)$ CST modality

Similarly in the case of external scanning with $\sigma = -1$, there may be a cut-off $\pi/2 < \omega_0 < \pi$, again the corresponding CLRT is the exterior $\mathcal{R}_{\mathcal{L}(s, \phi)}$ problem. The scanning circular arc is receding farther and it is necessary to stop somewhere with the cut-off ω_0 . Now for $s_{-1} = p |\tan \omega|$ with $\pi/2 < \omega < \pi$, we have also $0 < s_{-1} < \infty$. Hence we get a circular arc Radon transform in an annulus (or radii p and $p(\sqrt{1 + \tau^2} + \tau) > p$), which has an exact inversion solution by orthogonal functions expansion. See right image of Fig. 14.

6.2.3 In $(\sigma = 1, \epsilon = 1)$ CST modality

For the $\sigma = 0, 1$ modalities, a similar type of cut-off, near $\omega \sim 0$ or $\omega \sim \pi$ will correspond to a CLRT in an annular domain, for which no solution is known at present.

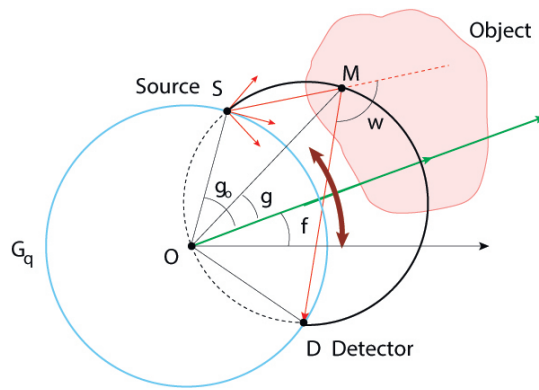


Figure 11: $\sigma = 0$ CST scanning modality for exterior object

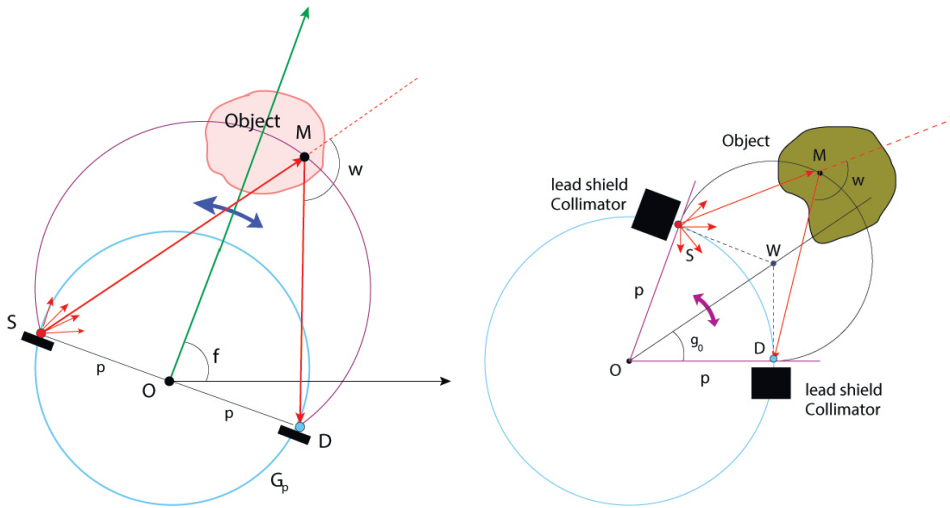


Figure 12: $\sigma = -1$ (left) and $\sigma = 1$ (right) CST scanning modalities for exterior object

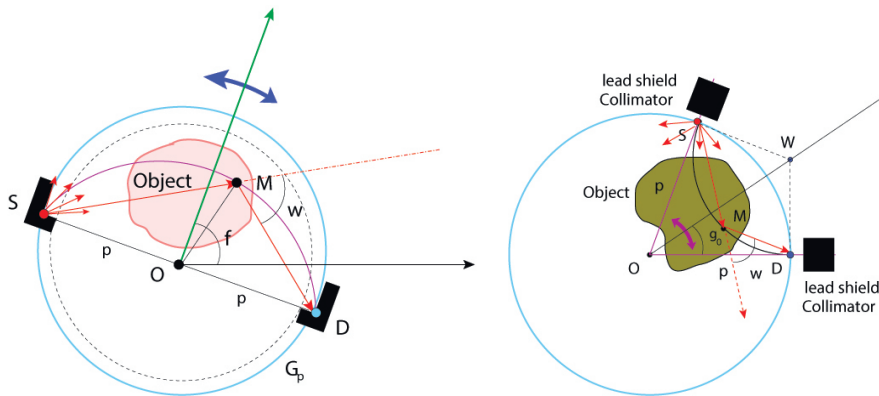


Figure 13: $\sigma = -1$ (left) and $\sigma = 1$ (right) CST scanning modalities for interior object

This is because $s_1 = \sin \omega$ for $\epsilon = \pm 1$ and $0 < s_1 < p$ for the full range of ω from 0 to π . However if we had a cut-off near $\omega \sim \pi/2$, then this missing data problem remains a CLRT interior problem, *albeit* re-scaled.

6.2.4 In $(\sigma = 0, \epsilon = 1)$ CST modality

Here $s_0 = p \cos \omega$ because $\omega = 2 \cos^{-1}(1/2\tau)$. Thus for $0 < \omega < \pi$, we have $0 < s_0 < p$. A cut-off around $\omega \sim 0$ would yield a re-scaled CLRT interior problem whereas a cut-off around $\omega \sim \pi$ would lead to a CLRT in an annular domain.

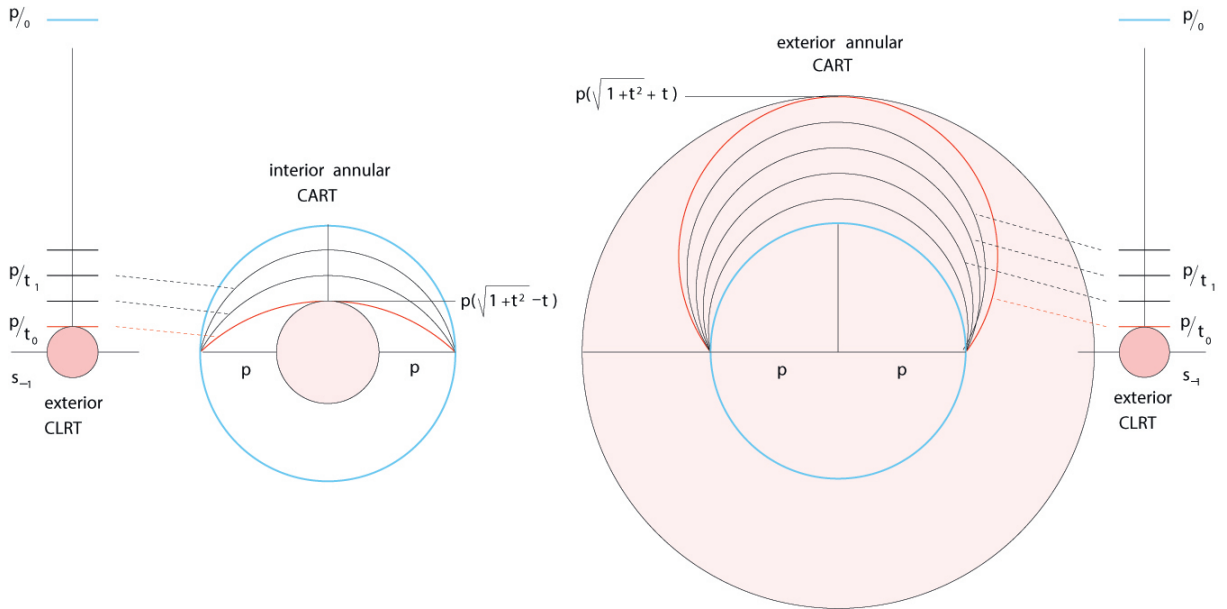


Figure 14: Representation of the incomplete data problem for CART with $\sigma = -1$ and $\epsilon = \pm 1$

6.3 Possibility for multiple modalities

The combination of $\mathcal{C}_0^1(p, \tau)$ and $\mathcal{C}_1^1(p, \tau)$ Radon transforms for external scanning, keeping S fixed and measuring at D scattered radiation flux density at two different energies may be viewed as a *bimodal* CST. This is easily realizable since all CST modalities obtained here have radiation source and detection running on the rim of the disk Γ_p . As the same electron density is reconstructed in any CST modality, this procedure differs from the usual bi-modal working where the attenuation map and the radio-tracer activity density are simultaneous reconstructed.

One may even operate all three $\epsilon = +1$ modalities on the same object simultaneously or all combinations of two $\epsilon = -1$ modalities simultaneously. This opens the possibility of producing images of higher quality since features that are missed in one modality may be recovered by another modality and put together at the end. In particular a bimodal modality with $\sigma = \pm 1$ and $\epsilon = -1$, would be advantageous in the region where $\omega \sim 0$, because the scanning will be performed with circular arcs of opposite concavity hence in a sense complementary information can be picked up.

6.4 Physical factors in realistic CST

6.4.1 Beam photometric spreading

Radiation from a point source has the tendency to spread as it propagates outward with a factor equal to the inverse square of the distance traveled: this is due to conservation of radiation flux during propagation from point source.

Proposition 6.1. *Let M be an arbitrary point on a $\mathcal{C}_\sigma^\epsilon(p, \tau)$ arc. Then the distances SM and DM verify*

$$SM^2 DM^2 = (p^2 - r^2)^2 \left(1 - \frac{\sigma}{\tau^2}\right). \quad (72)$$

Proof. In triangles OSM and ODM , write down the cosine identity

$$\begin{aligned} SM^2 &= p^2 + r^2 - 2pr \cos(\gamma_0 - \gamma) \\ DM^2 &= p^2 + r^2 - 2pr \cos(\gamma_0 + \gamma). \end{aligned} \quad (73)$$

It is understood that $r = r_{(\sigma, \epsilon)}$ for the five CST-relevant $\mathcal{C}_\sigma^\epsilon(p, \tau)$ arcs with the following data on (σ, ϵ) , τ and γ_0 given by the following table

(σ, ϵ)	γ_0	τ
$(-1, \pm 1)$	$\pi/2$	$0 < \tau < \infty$
$(0, 1)$	$\cos^{-1}(1/2\tau)$	$1/2 < \tau < \infty$
$(1, \pm 1)$	$\cos^{-1}(1/\tau)$	$1 < \tau < \infty$

Then eliminate γ from equation (73) to get the result of equation (72).

The CART on $\mathcal{C}_\sigma^\epsilon(p, \tau)$ arcs keep the main structure except $f(r, \theta)$ is replaced by $(p^2 - r^2)^{-2} \left(1 - \frac{\sigma}{\tau^2}\right)^{-1} f(r, \theta)$. The apparent divergence at $r = p$ is not real since the physical support of the function excludes these singularities. This has been reported for $(\sigma = \pm 1, \epsilon = \pm 1)$ in [6, 8].

6.4.2 Attenuation

This is a harder problem. Propagating radiation undergoes always attenuation, which is given by a function $a(r, \theta)$, which represents the coefficient of linear attenuation in the traversed medium and should be determined independently. However it modifies the structure of the expression of the CART, by multiplying the $\mathcal{C}_\sigma^\epsilon(p, \tau)$ arc integrand by a known function representing the attenuation on each linear radiation propagation path. This problem is not solved at present.

7 Conclusion

We have presented in this paper five classes of Radon transforms on circular arcs in the plane that are of interest for Compton Scatter Tomography. They all have a structure which can be converted back to one of the two classes of classical line Radon transform

problems: the *full plane* and the *interior* problems. This formidable advantage stems from the geometric fact that the circular arcs are all extracted from circles that have fixed power of the coordinate system origin. Among the many properties that can be transferred from the CLRT to the five CART is the solution to the function reconstruction problem either by explicit analytic inversion formulas or by orthogonal function expansions in the full plane or in a finite disk. In addition this transfer has brought up an elegant solution to the problem of incomplete data for some of the CART and has suggested some CST multiple-modality which could provide high quality tomographic images required in some applications.

Needless to say that future work perspectives include treatment of attenuated CART, possible extension in three dimensions (such as the one in [35]), development of finite versions of CART and conversion into efficient numerical algorithms for applications in medicine, non-destructive testing and evaluation as well as geological prospecting, etc.

Acknowledgments

The author is grateful to Professor V P Palamodov for pointing out the relevance of reference [22] to this work and for correspondence on this topic.

References

- [1] Radon J (1917) *Über die Bestimmung von Funktionen durch ihre Integralwerte längs gewisser Mannigfaltigkeiten* Ber.Verh.Sachs.Akad.Wiss. Leipzig-Math.-Natur.Kl. **69**: 262-77
- [2] Farmer F. T. & Collins M. P. (1971). *A new approach to the determination of anatomical cross-sections of the body by Compton scattering of gamma-rays*, Phys. Med. Biol. **16**(4): 577-586
- [3] Kondic N. N., (1978). *Density field determination by an external stationary radiation source using a kernel technique*, in Measurements in polyphase flows, papers of the ASME Winter Annual Meeting, D. E. Stock Ed., pp. 37-51, ASME, ISBN 9789993764281, San Francisco California USA, December 10-15, 1978.
- [4] Cormack A. M. (1964). *Representation of a function by its line integrals, with some radiological applications*, J. Appl. Phys **35**: 2908-2713.
- [5] Norton S. J., (1994). *Compton scattering tomography*, J. Appl. Phys. **76**: 2007-2015
- [6] Nguyen M K and Truong T T (2010) *Inversion of a new circular-arc Radon transform for Compton scattering tomography*, Inverse Problems **26**, 065005
- [7] Palamodov V P (2011) *An analytic reconstruction for the Compton scattering tomography in a plane*, Inverse Problems **27**, 125004
- [8] Truong T T and Nguyen M K (2011) *Radon transforms on generalized Cormack's curves and a new Compton scatter tomography modality*, Inverse Problems **27**, 125001
- [9] Truong T T and Nguyen M K (2012) *Recent Developments on Compton Scatter Tomography: Theory and Numerical Simulations*, in "Numerical Simulation - From Theory to Industry", Dr. Mykhaylo Andriychuk (Ed.), ISBN: 978-953-51-0749-1, InTech, DOI: 10.5772/50012.

-
- [10] Prettyman T. H., Gardner R. P., Russ J. C. & Verghese K., (1993). *A combined transmission and scattering tomographic approach to composition and density imaging*, Appl. Radiat. Isot. **44**(10/11): 1327-1341
- [11] Bodette D. E. & Jacobs A. M., (1985). *Tomographic two-phase flow distribution measurement using gamma-ray scattering*, ISA 1985, Paper 85-0362, pp. 23-34. ISSN 0019-0578
- [12] Evans B. L., Martin J. B., Burggraf L. W. & Roggemann M. C., (1998). *Nondestructive inspection using Compton scatter tomography*, IEEE Transactions on Nuclear Science **45**(3): 950-956
- [13] Cormack A. M. (1963). *Representation of a function by its line integrals, with some radiological applications*, J. Appl. Phys **34**: 2722-2727.
- [14] Verly J (1981) *Circular and extended circular harmonic transforms and their relevance to image reconstruction from line integrals*, Journal of the Optical Society of America **71**(7): 825-835
- [15] Hansen E W (1981) *Theory of circular harmonic image reconstruction*, J.Opt.Soc.Am., **71**(3): 304-308
- [16] Woods F S 1961 *Higher Geometry* (New-York: Dover)
- [17] Palamodov V P (2000) *Reconstruction from limited data of arc means*, The Journal of Fourier Analysis and Applications **6**(1): 25-42
- [18] Cormack A M (1981) *The Radon transform on a family of curves in the plane*, Proceedings of the American Mathematical Society **83**(2): 325-330
- [19] Quinto E T (1983) *Singular value decomposition and inversion methods for the exterior Radon transform and a spherical transform*, Journal of Mathematical Analysis and Applications **95**: 437-48
- [20] Yagle A E (1992) *Inversion of spherical means using geometric inversion and Radon transforms*, Inverse Problems **8**: 949-964
- [21] Denecker K, Van Overloop, and Sommen F (1998) *The general quadratic Radon transform*, Inverse Problems **14**(3): 615-633
- [22] Palamodov V P (2012) *A uniform reconstruction formula in integral geometry*, Inverse Problems **28**: 065014
- [23] Cormack A. M., (1984). *Radon's problem - Old and New*, SIAM - AMS Proceedings **14**: 33-39
- [24] Cormack A M (1982) *The Radon transform on a family of curves in the plane II*, Proceedings of the American Mathematical Society **86**(2): 293-298
- [25] Droste B (1983) *A new proof of the support theorem and the range characterization for the Radon transform*, Manuscripta math. **42**: 289-296
- [26] Ambartsoumian G, Gouia-Zarrad R and Lewis M A (2010) *Inversion of the circular Radon transform on an annulus*, Inverse Problems **26**: 105015
- [27] Helgason S (1965) *The Radon transform on Euclidean spaces, compact two-point homogeneous spaces and Grassmann manifolds*, Acta Mathematica **113**: 153-180
- [28] Ludwig D (1966) *The Radon transform on Euclidean space*, Communications in Pure and Applied Mathematics **19**: 49-81
- [29] Strichartz R S (1982) *Radon inversion - variations on a theme*, Amer. Math. Monthly **89**: 377-384

- [30] Perry R M (1977) *On reconstructing a function on the exterior of a disk from its Radon transform*, Journal of Mathematical Analysis and Applications **59**: 324-341
- [31] Magnus W, Oberhettinger F and Soni R P 1966 *Formulas and Theorems for the Special Functions of Mathematical Physics* 3rd Ed., Springer Verlag, Berlin.
- [32] Perry R M (1975) *Reconstruction of a function by circular harmonic analysis of its Radon transform*, in Digest of topical meeting on image processing for 2D and 3D reconstruction, Opt. Soc. Am., Washington.
- [33] Evans B. L., Martin J. B., Burggraf L. W., Roggemann M. C., and Hangartner T. N., (2002) *Demonstration of energy-coded Compton scatter tomography with fan beams for one-sided inspection*, Nuclear Instruments and methods in Physics Research A **480**: 797-806
- [34] Maass P (1991), *Singular value decompositions for the Radon transform*, in Mathematical Aspects of Computerized Tomography, Springer Lecture Notes in Mathematics **1497**: 6-14
- [35] Truong T T (2103) *Inversion of some spherical cap Radon transforms*, Eurasian Journal of Mathematical and Computer Applications **1**(1): 78-102

T.T. Truong,
Laboratoire de Physique Théorique et Modélisation,
UMR 8089 CNRS/Université de Cergy-Pontoise,
2 av. Adolphe Chauvin 95302 Cergy-Pontoise, France.
Email: truong@u-cergy.fr

Received 5 May 2014, in accepted 3 Jun 2014